Geophysical Research Letters

RESEARCH LETTER
10.1029/2019GL081961

Formation of a New Great Dark Spot on Neptune in 2018

A. A. Simon[1], **M. H. Wong**[2], **and A. I. Hsu**[2]

[1]NASA Goddard Space Flight Center, Solar System Exploration Division/690, Greenbelt, MD, USA, [2]Department of Astronomy, University of California, Berkeley, CA, USA

Key Points:
- Hubble images provide the first history of formation of a large, dark vortex on Neptune
- The vortex is similar in size and shape to the Voyager 2 Great Dark Spot and is drifting slower than the zonal wind speed
- The drift rate and likely precursor clouds in prior years are consistent with deep formation

Correspondence to:
A. A. Simon, and M. H. Wong,
amy.simon@nasa.gov;
mikewong@astro.berkeley.edu

Citation:
Simon, A. A., Wong, M. H., & Hsu, A. I. (2019). Formation of a new Great Dark Spot on Neptune in 2018. *Geophysical Research Letters*, *46*. https://doi.org/10.1029/2019GL081961

Received 8 JAN 2019
Accepted 14 FEB 2019

Abstract For the first time, Hubble Space Telescope visible-wavelength imaging shows the formation history of a dark vortex on Neptune. A new northern Great Dark Spot (NDS-2018) was discovered in September and November 2018 images, spanning roughly 12° of latitude and 27° in longitude (11,000 × 5,000 km) at 23°N planetographic latitude. NDS-2018 is similar in size, shape, and longitudinal drift rate as the Voyager 2 Great Dark Spot near 22°S. NDS-2018 was prominent in blue-wavelength November 2018 images and drifted at 2.46°/hr westward. Yearly global maps demonstrate possibly related cloud activity in prior years. The drift rate and formation history of the dark vortex indicates a deep origin. We estimate that the north-south gradient in zonal wind speed is almost 4 times larger at the depth of the dark vortex, compared with cloud-tracked zonal winds.

Plain Language Summary In 2018, a new Great Dark Spot was discovered on Neptune, nearly identical in size and shape as the one observed by Voyager 2 in 1989. The spot is in the Northern Hemisphere and is drifting westward more slowly than the surrounding winds. Dark spots can only be identified in visible light, because of their strong absorption at blue wavelengths, and only the Hubble Space Telescope has sufficient spatial resolution to detect them. A search of global Hubble Neptune images from 2015 through 2017 reveals smaller clouds present at locations consistent with this storm, meaning, it may take many years to form. If so, it may originate from much deeper in the atmosphere than previously thought. Future computer simulations of Neptune's dark storms can be constrained by these new observations to teach us more about deep atmosphere conditions and processes on all the giant planets.

1. Introduction

As part of the Hubble Outer Planet Atmosphere Legacy (OPAL) program, Neptune has been observed near Earth opposition on a yearly cadence since 2015 (Simon et al., 2015). The most recent OPAL Neptune observations in 2018 reveal a new, distinct, dark spot with bright companion clouds, centered on 23°N planetographic latitude. We use the name NDS-2018, for "northern dark spot discovered in 2018," following the naming convention of Hammel et al. (1995) and Wong et al. (2018). NDS-2018 is the sixth of a series of dark vortices discovered by Voyager and the Hubble Space Telescope (HST). These features are small with relatively low contrast, and they are visible only at blue/green wavelengths (e.g., Hammel et al., 1995, Wong et al., 2018). Observations of the properties and evolution of previous dark spots have led to new insights into the dynamics and structure of Neptune's atmosphere (e.g., Lebeau & Dowling, 1998, Sromovsky et al., 2001) and allowed quantitative comparison between large vortices seen in the atmospheres of all the giant planets.

But much remains mysterious about these features. No internal velocity field has been measured for any of Neptune's dark spots. The origin process has never been documented prior to this work. The demise of a dark vortex has only been documented for SDS-2015 in HST OPAL data (Wong et al., 2018) and possibly NDS-1994 during a period of intensive HST Neptune observations following the Voyager encounter (Sromovsky et al., 2001). Dark vortex lifetimes are mostly likely to be 2–3 years as constrained by HST data (Hsu et al., 2019), and OPAL may document the full lifetime of NDS-2018 if HST observes through 2021.

2. Observations

OPAL images are obtained at visible to near-infrared wavelengths with the Wide Field Camera 3 (WFC3/UVIS; Dressel, 2019), with the full Neptune filter list given in Wong et al. (2018). The observations are spaced to give two consecutive maps with global longitude coverage as Neptune rotates (16.11 hr), allowing the measurement of cloud motions. Images are mapped to longitude and latitude using ellipsoid limb fitting

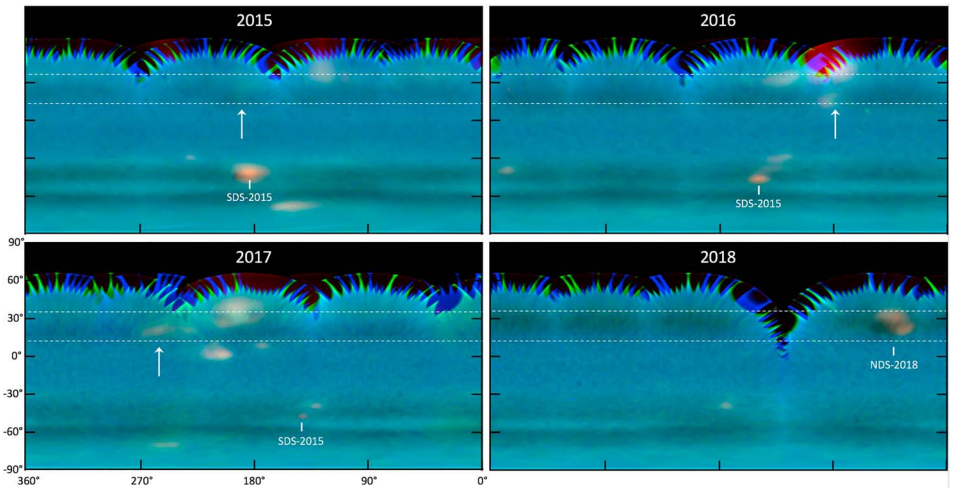

Figure 1. False-color global cylindrical maps from Hubble, spanning 180° of latitude and 360° of longitude, from images at 845 (red), 547 (green), and 467 nm (blue), and all use the same contrast scaling with a light unsharp mask applied. The maps are centered on 180°W longitude, except 2015, which was centered on 0° longitude. Dotted lines are shown at ~10° and 35°N to indicate the active region prior to the discovery of NDS-2018.

and synthetic image coregistration techniques and corrected for limb darkening at wavelengths below 800 nm using the Minnaert function (Simon et al., 2015; Wong et al., 2018).

In 2018, observations were first obtained on 10 September, but due to Hubble gyroscope problems, several orbits were truncated and significant coverage in the F467M filter was lost. In the images that were successfully acquired, there is some indication of a dark feature near midnorthern latitudes (Neptune's sub-Earth and subsolar point are both currently near 24°S latitude, limiting the view of the Northern Hemisphere) but only at one oblique view (Hsu et al., 2019). After HST's gyroscope operations were recovered, a full sequence of images was acquired on 5 and 6 November, covering two full Neptune rotations.

The darkest point within the dark spot falls at 23°N. However, the dark spot resides on the edge of a dark zonal band (Figure 1). The maximum contrast of the dark spot with respect to its surroundings at the same latitude is 10% at 20.8°N. Without a complete understanding of the nature of the aerosol structure within the dark spot and the dark zonal band, we take 23°N as the dynamical center of the feature.

OPAL's multiyear global maps provide monitoring capabilities that grow stronger with each year of new data (Figure 1), allowing us to track the long-term evolution of cloud systems. NDS-2018 appears at 48°W on 5 November (bottom right). In the false-color composite (467, 547, and 845 nm in B, G, and R, respectively), the companion clouds of NDS-2018 and SDS-2015 appear redder than other discrete cloud features, indicating differences between the aerosol vertical distributions of dark spot companion clouds compared to other discrete cloud features. However, both companion clouds and other discrete cloud features seen at visible wavelengths are thought to consist of methane ice particles (Smith et al., 1989; Sromovsky et al., 2001).

Short-time scale variation in companion cloud positioning and brightness is evident in maps of single frames from the November 2018 data, separated by about 19 hr (Figure 2, bottom row). Companion cloud brightness and coverage was greater in September 2018, and 2017 data showed no trace of a dark spot even though bright cloud features were present at the same latitude.

3. Drift Rate and Formation

Between 5 and 6 November, NDS-2018 moved about 47° in 19.07 hr, or 2.46°/hr (270 m/s). This drift rate extrapolates to a location of 308°W on 10 September, while the dark feature is observed at 339°W on that date. The longitude discrepancy could be the result of an error as small as 0.8% in the drift rate measured from the 5 and 6 November data or a small change in drift rate over the ~56-day interval between the observations, which is common among giant vortices (Smith et al., 1989; Wong et al., 2018). It is difficult to estimate the feature's location under a constant drift rate assumption in prior years, because very small errors in the drift rate can substantially change the extrapolated longitude of the feature over long time periods.

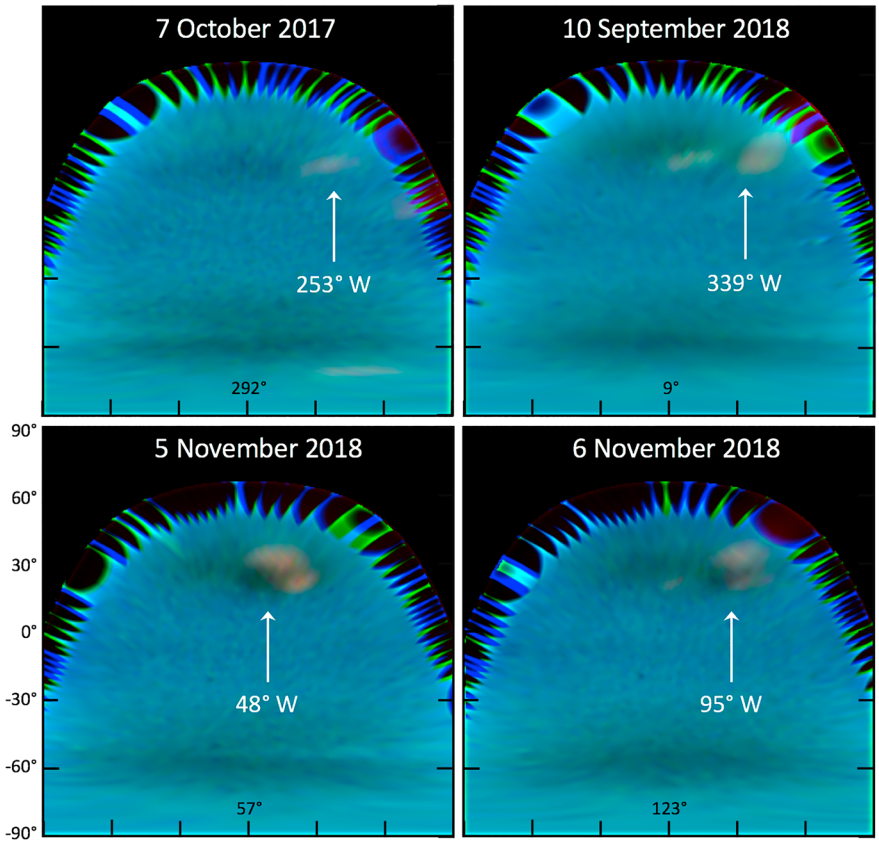

Figure 2. Individual maps from Hubble images in 2017 through 2018, in the same filters and processing as Figure 1. These maps span ±90° of latitude and longitude, and tick marks indicate 30° latitude and longitude intervals.

In each year of OPAL data, bright cloud features are seen in the active region at 10–35°N. Ground-based near-infrared observations in the 2017 time period also showed the presence of cloud activity spanning the 25–50°N region (Molter et al., 2019). We mark bright features as white arrows in Figure 1 and list the feature longitudes in Table 1. If we assume that these bright clouds mark the same feature from year to year, then we calculate drift rates very close to the 2.46°/hr drift rate measured for the dark spot itself in November 2018. Note that the zonal wind speed at 23°N is 311 m/s, or 2.81°/hr westward (Sromovsky et al., 1993), so the dark spot (and potentially the bright cloud features in 2015–2017) is drifting eastward with respect to the winds. In comparison, the Voyager 2 Great Dark Spot was located at 20°S, drifted at 2.73°/hr (Hammel et al., 1995; Smith et al., 1989).

We hypothesize that the 2016–2017 maps show cloud activity associated with the formation of NDS-2018 before the dark spot itself was visible. Although data sampled at an annual cadence are not sufficient to test this hypothesis, it is still clear that over these years, discrete regions of cloud activity were present on Neptune at the same latitude as NDS-2018, while all other longitudes within this band of activity lacked bright cloud features. The OPAL observations are able to reveal for the first time that enhanced cloud activity presaged the appearance of a dark spot by about 2 years. The SDS-2015 dark vortex may have shared a similar formation process, although it is likely that the onset of the OPAL program's Neptune observations in 2015 was too late to constrain the timing of its origin to within 1 year. The maximum contrast of SDS-2015 was about 6.7% in the F467M filter, and contrast decreased by about 1.7% per year over the 2015–2017 time period (Wong et al., 2018). If the 10% contrast of NDS-2018 is representative of the contrast of a freshly formed dark spot, then SDS-2015 could have been about 2 years old when first discovered by OPAL.

Table 1
Candidate Feature Measurements

Date	UTC	W. Longitude (deg)	Drift rate (deg/hr)[a]
2015-09-18	17.805	11	2.45
2016-10-04	0.558	87	2.46
2017-10-07	7.278	253	2.45
2018-09-10	2.160	339	2.44
2018-11-05	13.548	48	—
2018-11-06	8.622	95	2.46

[a]Drift rate assumes that the listed feature is the same feature as in 2018-11-05 observations

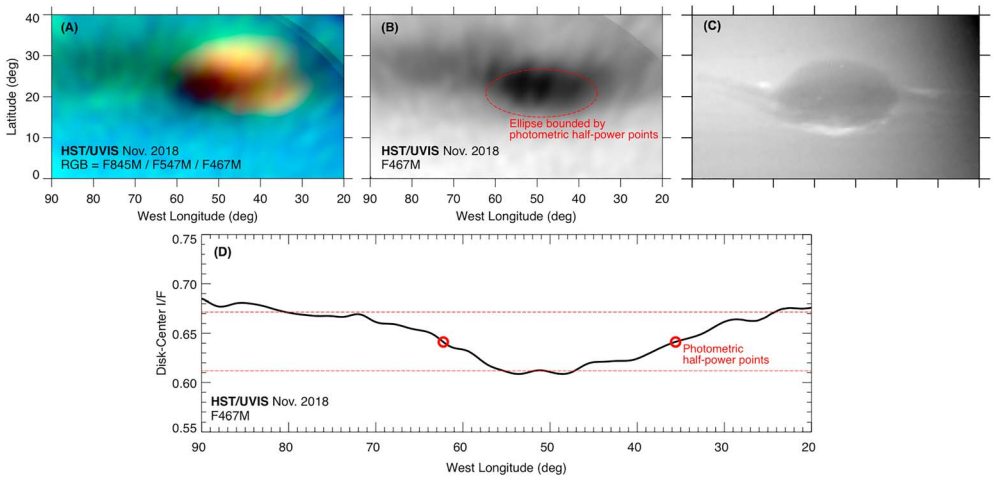

Figure 3. Morphology of NDS-2018 is shown in combined maps, aligned to the position at 13:33 UT on 5 November. Four map frames (corrected for limb darkening) were averaged in each filter, after shifting each entire map frame eastward according to the dark spot drift rate. Dark spot relative to companion clouds are shown in the false-color map (a), while the morphology of the dark spot is best revealed in the F467M filter (b). The spot is similar in size to the Voyager 2 Great Dark Spot (c), blue filter. The brightness profile of (b) is shown in (d). HST = Hubble Space Telescope.

SDS-2015 was discovered at 46°S in 2015, drifting to 49°S in 2017, with companion clouds offset to the north by 1–4° (Wong et al., 2018). Prior to its discovery, ground-based observations showed bright cloud features in 2014–2015 at latitudes of 35–45°S, while features in 2013 were spread over a wider range of 35–52°S (Hueso et al., 2017). Qualitatively, the observations suggest a similar formation process for NDS-2018 and SDS-2015. All previously observed dark spots were seen fully formed, with no record of their formation. SDS-2015 was observed through its demise, however, showing a slow poleward drift and diminishing size over several years (Figure 1; Wong et al., 2018).

4. Morphology and Wind Shear

To better constrain the morphology of the feature in November 2018, we combined four frames per filter, spanning two Neptune rotations (Figure 3). We used photometric half-power points in the east-west reflectivity profile, and the north-south contrast profile, to measure a size of 26.8° × 11.8° (11,000 × 5,000 km), with an aspect ratio of 2.2. The full width is similar to that of the Voyager 2 1989 Great Dark Spot (GDS) and the Hubble 1995 spot (Hammel et al., 1995; Smith et al., 1989).

Under a set of reasonable assumptions, the morphology of NDS-2018 suggests the presence of significant vertical wind shear on Neptune. The first assumption involves the intrinsic vorticity ζ_0 of the vortex, which cannot be directly measured. In fact, Voyager and HST imaging sequences have never been able to measure velocities within dark vortices. But studies of diverse vortices on Jupiter and Saturn (García-Melendo et al., 2007; Legarreta & Sánchez-Lavega, 2005; Sromovsky et al., 1993) show that most have intrinsic vorticities $\zeta_0 = (\zeta + f)/2$, where for NDS-2018 at 20.6°N, $f = 7.64 \times 10^{-5}$/s is the Coriolis parameter, and $\zeta = du/dy$ is the relative vorticity due to the zonal wind field. The second assumption, following from analysis of the properties of Neptune's GDS and Jupiter's Great Red Spot (Polvani et al., 1990), is that NDS-2018 obeys the Kida equations for a stationary vortex, relating the observed aspect ratio and the vorticity of the dark spot to the north-south gradient of the zonal winds, du/dy (Kida, 1981):

$$\zeta/\zeta_0 = (1-\lambda)/(\lambda(1+\lambda)), \tag{1}$$

where λ is the reciprocal aspect ratio of the vortex b/a. We can then determine the relative vorticity in the vortex environment as a function vortex aspect ratio:

$$\zeta = f(1-\lambda)/(2\,\lambda(1+\lambda)-(1-\lambda)). \tag{2}$$

Figure 4 plots equation (2) as a black line, and the aspect ratio measured from the HST images is shown as a blue bar centered at $a/b = 2.2$. The intersection of these suggests that $\zeta = du/dy$ is 5.5×10^{-5}/s in the

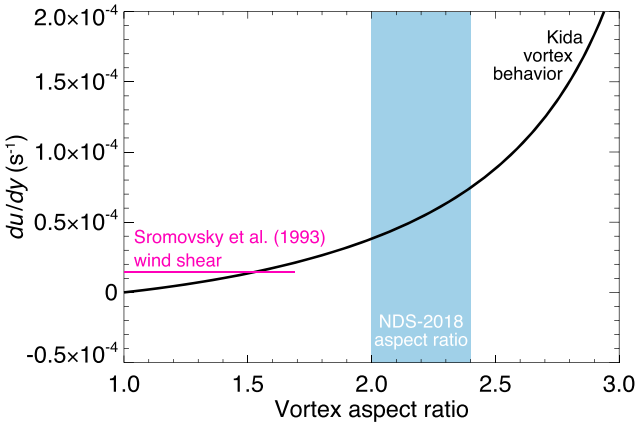

Figure 4. The vortex aspect ratio may reveal vertical wind shear below the visible clouds. An aspect ratio of 2.2 (Figure 3) corresponds to a zonal wind gradient of $du/dy = 5.4 \times 10^{-5}$/s (intersection of blue bar and black curve; see text for underlying assumptions). This is almost 4 times larger than the gradient of 1.5×10^{-5}/s (pink line) from Voyager cloud-tracked winds (Sromovsky et al., 1993). The differing values of du/dy could be consistent if there is vertical wind shear, and the vortex center of mass lies deeper than the cloud-tracked winds.

environment of the vortex, about a factor of 4 larger than the gradient measured in the cloud-tracked winds from Voyager data (Sromovsky et al., 1993), shown as a pink line. Since dark vortices are thought to be deep phenomena (compared to the observed methane ice clouds), the difference between the vortex-derived du/dy and the cloud-tracked winds requires a vertical gradient if all our assumptions hold true (de Pater et al., 2014).

Testing these assumptions is difficult, however. The strongest indication that the Kida equations govern dark vortex dynamics is from Voyager time sequences showing the oscillation in shape of the GDS, but acquiring similar time series for new dark vortices may not be possible until the next spacecraft mission to Neptune. Internal velocities currently cannot be measured within dark vortices, but such measurements are needed to test our original assumption that $\zeta_0 = (\zeta + f)/2$ for NDS-2018 and other dark vortices. Until measurement capabilities increase at a future date, our results are suggestive of vertical wind shear but not definitive.

5. Discussion

OPAL observations show that the appearance of NDS-2018 (like SDS-2015) was preceded by increased cloud activity throughout the region, with 2 to 3 years of activity prior to the visibility of the dark spot. Although numerical models have never been created to simulate the origin of Neptune's anticyclones, models have demonstrated a positive correlation between vortex depth and companion cloud brightness (Stratman et al., 2001). Bright clouds in 2016–2017, followed by lower-opacity clouds once the dark spot was directly visible, are consistent with a formation that involves a gradual increase in altitude of the vortex. But this scenario is challenging to reconcile with the suggestion of a near-constant drift rate (Table 1), because vertical wind shear should influence vortex drift rate (Legarreta & Sánchez-Lavega, 2005), as changes in height alter the influence of surrounding winds on the vortex. On the other hand, shear instability may form giant vortices and should also be further investigated.

Winds on Neptune have been measured by tracking methane ice clouds in Voyager images (Hammel et al., 1995; Limaye & Sromovsky, 1991; Smith et al., 1989), in HST images (Hammel & Lockwood, 1997; Karkoschka, 2011), and in ground-based infrared images with adaptive optics (Fitzpatrick et al., 2014; Martin et al., 2012). Significant dispersion in the zonal wind profile has been seen. A wavelength dependence in the infrared data suggests that some of the dispersion is due to vertical wind shear (Tollefson et al., 2018). Dark spot drift rates and aspect ratios provide key evidence that the vertical gradient extends to deeper levels, where winds cannot be directly measured by remote sensing. Our results suggest that du/dy at the vortex midplane is greater than at the methane ice cloud level, but without knowledge of the vertical extent of the vortex, we cannot quantitatively measure the vertical wind shear. Future studies of vertical wind shear will be valuable for future atmospheric entry probe mission design, influencing descent rates and entry latitudes.

Neptune may be unique among the giant planets, in that precursor hints of the still-forming vortex are visible and are not blocked by dense clouds (Jupiter) or hazes (Saturn and Uranus), giving a much better indication of a long formation process. This combined, with the drift and aspect ratio measurements, provide critical constraints on general circulation modeling. Although ground-based facilities can map bright cloud features, Hubble is the only currently operating facility with the demonstrated capability to detect these small, low-contrast dark spots at blue wavelengths. The OPAL program has enabled ground-breaking new constraints to be placed on the evolution of these features, including the first documentation of the origin of a dark vortex on Neptune.

Acknowledgments
This work used data acquired from the NASA/ESA Hubble Space Telescope, associated with OPAL program (PI: Simon, GO13937), and archived by the Space Telescope Science Institute, which is operated by the Association of Universities for Research in Astronomy, Inc., under NASA contract NAS 5-26555. All OPAL maps are available at https://doi.org/10.17909/T9G593, and we acknowledge financial support from this program and from program GO-14492. We thank Agustin Sánchez-Lavega for helpful discussions.

References

de Pater, I., Fletcher, L., Luszcz-Cook, S., DeBoer, D., Butler, B., Hammel, H. B., et al. (2014). Neptune's global circulation deduced from multi-wavelength observations. *Icarus*, *237*, 211–238. https://doi.org/10.1016/j.icarus.2014.02.030
Dressel, L. (2019). *Wide Field Camera 3 instrument handbook*, Version 11.0. Baltimore, MD: STScI.

Fitzpatrick, P. J., de Pater, I., Luszcz-Cook, S., Wong, M. H., & Hammel, H. B. (2014). Dispersion in Neptune's zonal wind velocities from NIR Keck AO observations in July 2009. *Astrophysics and Space Science*, *350*(1), 65–88. https://doi.org/10.1007/s10509-013-1737-2

García-Melendo, E., Sánchez-Lavega, A., & Hueso, R. (2007). Numerical models of Saturn's long-lived anticyclones. *Icarus*, *191*(2), 665–677. https://doi.org/10.1016/j.icarus.2007.05.020

Hammel, H. B., & Lockwood, G. W. (1997). Atmospheric structure of Neptune in 1994, 1995, and 1996: HST imaging at multiple wavelengths. *Icarus*, *129*(2), 466–481. https://doi.org/10.1006/icar.1997.5764

Hammel, H. B., Lockwood, G. W., Mills, J. R., & Barnet, C. D. (1995). Hubble Space Telescope imaging of Neptune's cloud structure in 1994. *Science*, *268*(5218), 1740–1742. https://doi.org/10.1126/science.268.5218.1740

Hsu, A. I., Wong, M. H., & Simon, A. A. (2019). Lifetimes and occurrence rates of dark vortices on Neptune from 23 years of Hubble Space Telescope images. *Astronomical Journal*. https://doi.org/10.3847/1538-3881/ab0747

Hueso, R. A., de Pater, I., Simon, A., Sánchez-Lavega, A., Delcroix, M., Wong, M. H., et al. (2017). Neptune long-lived atmospheric features in 2013–2015 from small (28-cm) to large (10-m) telescopes. *Icarus*, *295*, 89–109. https://doi.org/10.1016/j.icarus.2017.06.009

Karkoschka, E. (2011). Neptune's rotational period suggested by the extraordinary stability of two features. *Icarus*, *215*(1), 439–448. https://doi.org/10.1016/j.icarus.2011.05.013

Kida, S. (1981). Motion of an elliptic vortex in a uniform shear flow. *Journal of the Physical Society of Japan*, *50*(10), 3517–3520. https://doi.org/10.1143/JPSJ.50.3517

Lebeau, R. P., & Dowling, T. E. (1998). EPIC simulations of time-dependent, three-dimensional vortices with application to Neptune's Great Dark Spot. *Icarus*, *132*(2), 239–265. https://doi.org/10.1006/icar.1998.5918

Legarreta, J., & Sánchez-Lavega, A. (2005). Jupiter's cyclones and anticyclones vorticity from Voyager and Galileo images. *Icarus*, *174*(1), 178–191. https://doi.org/10.1016/j.icarus.2004.10.006

Limaye, S. S., & Sromovsky, L. A. (1991). Winds of Neptune: Voyager observations of cloud motions. *Journal of Geophysical Research*, *96*(S01), 18941. https://doi.org/10.1029/91JA01701

Martin, S. C., de Pater, I., & Marcus, P. (2012). Neptune's zonal winds from near-IR Keck adaptive optics imaging in August 2001. *Astrophysics and Space Science*, *337*(1), 65–78. https://doi.org/10.1007/s10509-011-0847-y

Molter, E. M., de Pater, I., Luszcz-Cook, S., Hueso, R., Tollefson, J., Alvarez, C., et al. (2019). Analysis of Neptune's 2017 bright equatorial storm. *Icarus*, *321*, 324–345. https://doi.org/10.1016/j.icarus.2018.11.018

Polvani, L. M., Wisdom, J., Dejong, E., & Ingersoll, A. P. (1990). Simple dynamical models of Neptune's Great Dark Spot. *Science*, *249*(4975), 1393–1398. https://doi.org/10.1126/science.249.4975.1393

Simon, A. A., Wong, M. H., & Orton, G. S. (2015). First results from the Hubble Opal Program: Jupiter in 2015. *Astrophysical Journal*, *812*(1), 55. https://doi.org/10.1088/0004-637X/812/1/55

Smith, B. A., Soderblom, L., Banfield, D., Barnet, C., Basilevsky, A. T., Beebe, R. F., et al. (1989). Voyager 2 at Neptune: Imaging science results. *Science*, *246*(4936), 1422–1449. https://doi.org/10.1126/science.246.4936.1422

Sromovsky, L. A., Fry, P., Dowling, T., Baines, K., & Limaye, S. (2001). Neptune's atmospheric circulation and cloud morphology: Changes revealed by 1998 HST imaging. *Icarus*, *150*(2), 244–260. https://doi.org/10.1006/icar.2000.6574

Sromovsky, L. A., Limaye, S., & Fry, P. (1993). Dynamics of Neptune's major cloud features. *Icarus*, *105*(1), 110–141. https://doi.org/10.1006/icar.1993.1114

Stratman, P. W., Showman, A., Dowling, T., & Sromovsky, L. (2001). EPIC simulations of bright companions to Neptune's Great Dark Spots. *Icarus*, *151*(2), 275–285. https://doi.org/10.1006/icar.2001.6603

Tollefson, J., de Pater, I., Marcus, P. S., Luszcz-Cook, S., Sromovsky, L. A., Fry, P. M., et al. (2018). Vertical wind shear in Neptune's upper atmosphere explained with a modified thermal wind equation. *Icarus*, *311*, 317–339. https://doi.org/10.1016/j.icarus.2018.04.009

Wong, M. H., Tollefson, J., Hsu, A., de Pater, I., Simon, A. A., Hueso, R., et al. (2018). A new Dark Vortex on Neptune. *Astronomical Journal*, *155*(3), 117. https://doi.org/10.3847/1538-3881/aaa6d6